selected by the following criteria: (1) stable intertrial baseline, without statistically significant differences in average firing rate between pre-low-tone and pre-high-tone baselines (the overall average baseline firing for the 94 cells was 10.03 spike s^{-1}; and (2) statistically significant differences in firing between the two tones, at tone presentation or in the subsequent delay. These cells were submitted to the correlational analysis of average tone- and colour-related differences (deltas) between trial periods. Four such periods were the object of analysis: (1) first 1 s of tone; (2) 10-s delay; (3) first 1 s of colour presentation; and (4) 400-ms period immediately preceding manual choice of colour. Tone and colour periods (1, 3 and 4) were divided in 200-ms bins, and the entire delay period was treated as a 10-s bin. Four tone- or colour-related differences or deltas (Fig. 2e) were determined between high-tone (red choice) trials and low-tone (green choice) trials: Δ_1 (tone), largest 1-bin difference between responses to the two tones; Δ_2 (delay), tone-related difference in delay firing; Δ_3 (colours), largest 1-bin difference in response to the two simultaneous colours; and Δ_4 (chosen colour), largest 1-bin difference in pre-choice firing. Table 1 tabulates cells by correlation of delta sign across trial periods. Figure 4a, b shows delta correlations by magnitude. Expected correlations by chance were calculated by shuffling 1,000 times the delta values from both animals (94 differential units) in correct-response trials: the mean coefficient (r) thus obtained for all four interperiod correlations (Δ_1 versus Δ_2, Δ_3 versus Δ_2, Δ_3 versus Δ_1, and Δ_4 versus Δ_1) ranged between minus 0.002 and plus 0.003 (s.d. 0.103–0.105).

Received 15 February; accepted 29 March 2000.

1. Luria, A. R. *Higher Cortical Functions in Man* (Basic Books, New York, 1966).
2. Fuster, J. M. *The Prefrontal Cortex* 3rd edn (Lippincott–Raven, Philadelphia, 1997).
3. Jones, E. G. & Powell, T. P. S. An anatomical study of converging sensory pathways within the cerebral cortex of the monkey. *Brain* **93,** 793–820 (1970).
4. Pandya, D. N. & Yeterian, E. H. in *Cerebral Cortex* (eds Peters, A. & Jones, E. G.) 3–61 (Plenum, New York, 1985).
5. Romanski, L. M. *et al.* Dual streams of auditory afferents target multiple domains in the primate prefrontal cortex. *Nature Neurosci.* **2,** 1131–1136 (1999).
6. Fuster, J. M. Unit activity in prefrontal cortex during delayed-response performance: Neuronal correlates of transient memory. *J. Neurophysiol.* **36,** 61–78 (1973).
7. Niki, H. Differential activity of prefrontal units during right and left delayed response trials. *Brain Res.* **70,** 346–349 (1974).
8. Funahashi, S., Bruce, C. J. & Goldman-Rakic, P. S. Mnemonic coding of visual space in the monkey's dorsolateral prefrontal cortex. *J. Neurophysiol.* **61,** 331–349 (1989).
9. Bodner, M., Kroger, J. & Fuster, J. M. Auditory memory cells in dorsolateral prefrontal cortex. *NeuroReport* **7,** 1905–1908 (1996).
10. Romo, R., Brody, C. D., Hernández, A. & Lemus, L. Neuronal correlates of parametric working memory in the prefrontal cortex. *Nature* **399,** 470–473 (1999).
11. Fuster, J. M., Bauer, R. H. & Jervey, J. P. Cellular discharge in the dorsolateral prefrontal cortex of the monkey in cognitive tasks. *Exp. Neurol.* **77,** 679–694 (1982).
12. Rao, S. C., Rainer, G. & Miller, E. K. Integration of what and where in primate prefrontal cortex. *Science,* **276,** 821–824 (1997).
13. Rainer, G., Asaad, W. F. & Miller, E. K. Selective representation of relevant information by neurons in the primate prefrontal cortex. *Nature* **393,** 577–579 (1998).
14. Watanabe, M. Reward expectancy in primate prefrontal neurons. *Nature* **382,** 629–632 (1996).
15. Petrides, M. & Pandya, D. N. in *Handbook of Neuropsychology* (eds Boller, F. & Grafman, J.) 17–58 (Elsevier, Amsterdam, 1994).
16. Wilson, F. A. W., Scalaidhe, S. P. O. & Goldman-Rakic, P. S. Dissociation of object and spatial processing domains in primate prefrontal cortex. *Science* **260,** 1955–1958 (1993).
17. Desimone, R., Albright, T. D., Gross, C. G. & Bruce, C. Stimulus-selective properties of inferior temporal neurons in the macaque. *J. Neurosci.* **4,** 2051–2062 (1984).
18. Miyashita, Y. Neuronal correlate of visual associative long-term memory in the primate temporal cortex. *Nature* **335,** 817–820 (1988).
19. Iwamura, Y., Tanaka, M., Sakamoto, M. & Hikosaka, O. Rostrocaudal gradients in the neuronal receptive field complexity in the finger region of the alert monkey's postcentral gyrus. *Exp. Brain Res.* **92,** 360–368 (1993).
20. Tanaka, K. Neuronal mechanisms of object recognition. *Science* **262,** 685–688 (1993).
21. Colombo, M. & Gross, C. G. Responses of inferior temporal cortex and hippocampus neurons during delayed matching to sample in monkeys (*Macaca fascicularis*). *Behav. Neurosci.* **108,** 443–455 (1994).
22. Gibson, J. R. & Maunsell, J. H. R. Sensory modality specificity of neural activity related to memory in visual cortex. *J. Neurophysiol.* **78,** 1263–1275 (1997).
23. Hikosaka, K., Iwai, E., Saito, H. & Tanaka, K. Polysensory properties of neurons in the anterior bank of the caudal superior temporal sulcus of the macaque monkey. *J. Neurophysiol.* **60,** 1615–1637 (1988).
24. Zhou, Y. & Fuster, J. M. Neuronal activity of somatosensory cortex in a cross-modal (visuo-haptic) memory task. *Exp. Brain Res.* **116,** 551–555 (1997).
25. Fuster, J. M., Bauer, R. H. & Jervey, J. P. Functional interactions between inferotemporal and prefrontal cortex in a cognitive task. *Brain Res.* **330,** 299–307 (1985).
26. Wise, S. P., Boussaoud, D., Johnson, P. B. & Caminiti, R. Premotor and parietal cortex: corticocortical connectivity and combinatorial computations. *Annu. Rev. Neurosci.* **20,** 25–42 (1997).
27. Tomita, H., Ohbayashi, M., Nakahara, K., Hasegawa, I. & Miyashita, M. Top-down signal from prefrontal cortex in executive control of memory retrieval. *Nature* **401,** 699–703 (1999).
28. Matelli, M., Luppino, G. & Rizzolatti, G. Patterns of cytochrome oxidase activity in the frontal agranular cortex of macaque monkey. *Behav. Brain Res.* **18,** 125–137 (1985).
29. Petrides, M. The effect of periarcuate lesions in the monkey on the performance of symmetrically and asymmetrically reinforced visual and auditory go, no-go tasks *J. Neurosci.* **6,** 2054–2063 (1986).
30. Fuster, J. M. & Jervey, J. P. Neuronal firing in the inferotemporal cortex of the monkey in a visual memory task. *J. Neurosci.* **2,** 361–375 (1982).

Acknowledgements

We thank W. Bergerson and B. Lubell for technical assistance; L. Fairbanks for statistical counsel; and C. R. Gallistel, J. Maunsell, W. T. Newsome, T. Sejnowski and Y. Zhou for valuable comments on the manuscript. This work was supported by grants from the National Institute of Mental Health.

Correspondence and requests for materials should be addressed to J.M.F. (e-mail: joaquinf@ucla.edu).

Phenotypic suppression of *empty spiracles* is prevented by *buttonhead*

Frieder Schöck*†, Joachim Reischl‡, Ernst Wimmer‡, Heike Taubert*, Beverly A. Purnell*† & Herbert Jäckle*

* *Max-Planck-Institut für Biophysikalische Chemie, Abt. Molekulare Entwicklungsbiologie, Am Fassberg 11, 37077 Göttingen, Germany*
‡ *Lehrstuhl für Genetik, Universität Bayreuth, Universitätsstr. 30, NW1, 95440 Bayreuth, Germany*

Unlike the trunk segments, the anterior head segments of *Drosophila* are formed in the absence of pair-rule[1,2] and HOX-cluster gene[3] expression, by the activities of the gap-like genes *orthodenticle* (*otd*), *empty spiracles* (*ems*) and *buttonhead* (*btd*)[4,5]. The products of these genes are transcription factors[6,7], but only EMS has a HOX-like homeodomain[8,9]. Indeed, *ems* can confer identity to trunk segments[10] when other HOX-cluster gene activities are absent[3,11]. In trunk segments of wild-type embryos, however, *ems* activity is prevented by phenotypic suppression[10], in which more posterior HOX-cluster genes inactivate the more anterior without affecting transcription or translation[12]. *ems* is suppressed by all other Hox-cluster genes and so is placed at the bottom of their hierarchy[10]. Here we show that misexpression of EMS in the head transforms segment identity in a *btd*-dependent manner, that misexpression of BTD in the trunk causes *ems*-dependent structures to develop, and that EMS and BTD interact *in vitro*. The data indicate that this interaction may allow *ems* to escape from the bottom of the HOX-cluster gene hierarchy and cause a dominant switch of homeotic prevalence in the anterior–posterior direction.

Combined activities of *otd*, *ems* and *btd*[5] generate and specify *Drosophila* head segments (Fig. 1a–d) in the absence of pair-rule and homeotic gene activities[4] (Fig. 1e). *btd* alone is required for development of the mandibular segment, *btd* plus *ems* for the intercalary segment, and *btd*, *ems* plus *otd* for the antennal segment (Fig. 1e). Misexpression of *btd* or *otd* in the prospective head region failed to cause homeotic transformations[13,14] showing that neither of the two genes carries the proposed homeotic function in head segmentation[5]. To explore the untested homeotic role of *ems* and to address a possible cooperation with *btd*, we misexpressed the *ems* protein (EMS) in the *btd* domain of otherwise wild-type embryos. EMS expression was achieved by an *ems* complementary DNA transgene under control of the *btd cis*-acting promoter region[13].

EMS expression in the *btd* domain of wild-type embryos caused a second intercalary-like *engrailed* expression domain in place of the mandibular segment (Fig. 2a and d). Furthermore, these embryos developed a duplicate set of intercalary cuticle elements in place of mandibular structures (compare Fig. 2b, c with e, f). We observed the same results in response to EMS expression in the anterior third of blastoderm embryos mediated by a Gal4/UAS system[15]. However, misexpression of OTD in the *btd* domain had no effect on head

† Present addresses: Department of Genetics, Harvard Medical School, 200 Longwood Avenue, Boston, Massachusetts 02115, USA (F.S.); American Association for the Advancement of Science, 1200 New York Avenue NW, Washington DC 20005, USA (B.A.P).

formation (data not shown). Thus, among the three head gap-like genes only *ems* carries both early segmentation and homeotic selector gene function. However, *ems* misexpression in several head segments caused only the mandibular into intercalary segment transformation. As the intercalary segment also depends on *btd*, and *ems* did not have transforming activity in *btd* mutant embryos (data not shown), we conclude that *ems* activity is able to specify head segment identity only when acting in concert with *btd*. Notably, the direction of the *ems*-dependent transformation is from a posterior into a more anterior segment identity. This is opposite to the direction of transformation in response to ectopically expressed HOX-cluster genes in the trunk (reviewed in ref. 12).

BTD is a transcriptional activator with *in vitro* properties that are indistinguishable from those of human Sp1 (refs 7,16). However, whereas transgene-derived *btd* activity causes a full rescue of all head segments that are deleted in *btd* mutant embryos[7,16], Sp1 activity could rescue only mandibular segment development. Similarly, expression of the fusion protein VP16^{BTDzf}, which contains the VP16 transactivator region[17] fused to BTD's zinc finger domain[7], only rescued mandibular development (Fig. 3a; Fig. 2g–i). Conversely, expression of BTD^{Sp1zf}, in which the BTD zinc finger domain was replaced by the zinc finger domain of human Sp1, mediated a complete rescue of *btd* mutant embryos (Fig. 3a). Thus, BTD must contain specific features outside its zinc finger domain that are needed for intercalary segment development.

To identify the BTD region necessary for the *ems*-dependent intercalary development, we then asked whether BTD can physically interact with EMS *in vitro* and which parts of BTD are involved. BTD is able to bind [^{35}S]methionine-labelled EMS *in vitro* (Fig. 3b). This interaction involves the amino-terminal region of the protein (Fig. 3c and d). We could not define a specific domain as several parts of the N-terminal region interacted with EMS (Fig. 3e and f), excluding the zinc finger domain (not shown). Sp1, which has the same biochemical features as BTD[16], failed to interact with EMS (data not shown). The yeast two-hybrid system also showed a direct interaction between EMS and BTD's N-terminal region that does not involve the homeodomain of EMS (Fig. 3g and h).

Next we examined whether the BTD mutants that interact with EMS were sufficient to allow homeotic EMS activity *in vivo*. We performed transgene-dependent rescue experiments in which BTD deletion mutants were expressed in *btd* mutant embryos. N–BTD, a protein composed of the combined DNA-binding and N-terminal region, rescues all head segments of *btd* mutant embryos, whereas C–BTD, a protein lacking the N terminus, causes mandibular segment development in all *btd* mutant embryos but restores only partial intercalary development in rare cases (<5%; $n = 66$ embryos; Fig. 3a). Furthermore, BTD variants that lack various portions of the N terminus were able to restore intercalary segment development fully, indicating that BTD-dependent intercalary development depends on the parts of its N-terminal region that also allow physical interaction with EMS.

To investigate whether the BTD and EMS interaction causes homeotic transformations in other parts of the embryo, we made use of the observation that *ems* is also expressed in the trunk region of the embryo from stage 9 onwards[8,9]. Lack of *ems* activity causes no alteration in trunk segments except that the 'filzkörper', a morpho-

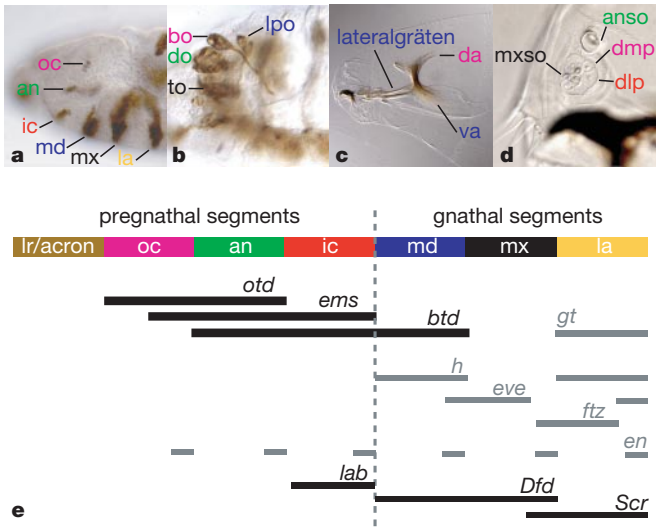

Figure 1 Representation of the *Drosophila* head. **a**, **b**, Heads of wild-type embryos showing segmental stripes of Engrailed (**a**) and larval head sensory organs stained with 22C10 monoclonal anitbody (**b**). **c**, **d**, Cuticle head markers of larvae (**c**) including the antennomaxillary complex (enlarged; **d**). Segmental origin is labelled according to the colour code shown in **e**. Note the Bolwig organ (bo), the dorsal arms (da) and the dorsomedial papilla (dmp) (ocular segment), the antennal sense organ (anso) and the dorsal organ (do) (antennal segment), the dorsolateral papilla (dlp) (intercalary segment), the lateropharyngeal organ (lpo) and ventral arms (va) (mandibular segment), the maxillary sense organ (mxso) and the terminal organ (to) (maxillary segment). For details see ref. 26. **e**, The head anlage showing the position and colour code for labial (la), maxillary (mx), mandibular (md), intercalary (ic), antennal (an), ocular (oc) segments and the labrum (lr) as part of the acron[27]. Black bars, blastoderm expression domains of *orthodenticle* (*otd*), *empty spiracles* (*ems*), *buttonhead* (*btd*) and the homeotic genes *labial (lab)*, *Deformed (Dfd) and Sex combs reduced (Scr)*; grey bars, expression domains of *giant* (*gt*), the pair-rule genes *hairy* (*h*), *even-skipped* (*eve*) and *fushi tarazu* (*ftz*) and the segment polarity gene *engrailed* (*en*).

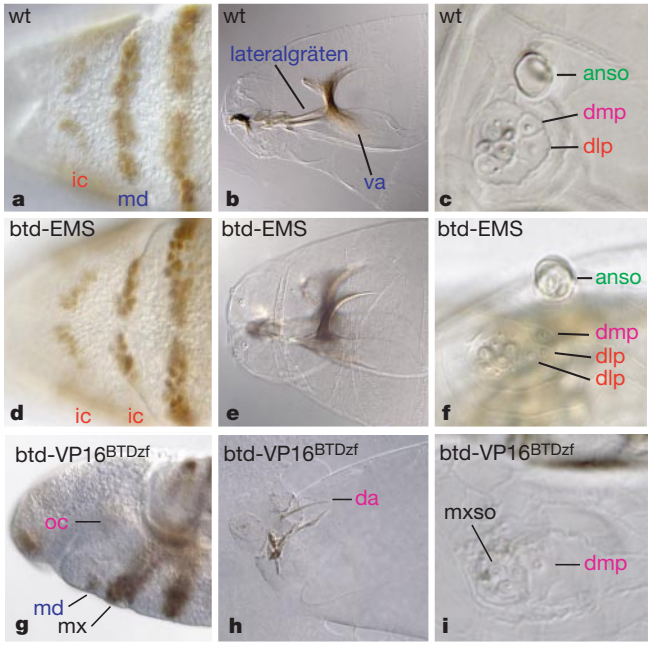

Figure 2 Misexpression of *ems* in the *btd* domain of wild-type embryos transforms mandibular to intercalary identity. **a**–**c**, Wild-type embryos. **a**, Mandibular (md) and intercalary (ic) Engrailed stripes (ventral view). **b**, Head skeleton. **c**, Antennomaxillary complex with a single dorsolateral papilla (dlp) of intercalary origin. **d**–**f**, Corresponding embryos containing two copies of the btd–EMS construct. **d**, The two most anterior Engrailed stripes showing the characteristics of the intercalary Engrailed stripe. **e**, Mandibular skeleton structures (ventral arms and lateralgräten)[7] are reduced and absent, respectively. **f**, Duplicated dlp indicates intercalary structures at the expense of mandibular development. Controls confirmed that OTD does not cause transformations when acting with EMS and/or BTD in the intercalary segment anlage[13,14]. **g**–**l**, Transgene-dependent rescue of *btd*-dependent mandibular segment by VP16^{BTDzf} expression in *btd* mutants (see text) is similar to the Sp1-dependent rescue[13]. Note a reduced mandibular Engrailed stripe (**g**), the head skeleton including dorsal arms (da; **h**) and the antenno-maxillary complex lacking dlp and anso (**i**). For comparison see Fig. 1a–d.

logically distinct structure of the last abdominal segment[18], fails to develop. In the absence of all HOX-cluster gene activities, however, the trunk segments alter identity and develop *ems*-dependent sclerotic head plates[10]. Their formation can be phenotypically suppressed by the co-expression of any gene of the HOX-cluster including *labial, Deformed* or *Sex combs* reduced[10], which are normally expressed and required in the cephalic region of the embryo (Fig. 1e; reviewed in ref. 3). Therefore, *ems* may be a disconnected member of the ancient HOX-cluster[3,11], acting at the bottom of the functional HOX-cluster hierarchy[10].

The *ems*-dependent homeotic transformation in the head region may be because of a requirement of EMS to cooperate with BTD to escape from phenotypic suppression. To test this in the trunk region, we expressed BTD from a heat-shock-inducible transgene at various early embryonic stages. Ectopic BTD expression up to and during blastoderm stage had no effect on trunk segmentation (data not shown). However, BTD expression during stage 7–9 of embryogenesis, when *ems* is initially expressed in the prospective trunk region[8,9], caused a range of phenotypes. These included the development of sclerotic head plates reminiscent of the *ems*-dependent structures observed in embryos that lack the HOX-cluster genes[10].

Most BTD misexpressing embryos develop fusions of trunk segments to varying degrees (149 cases out of 218 heat-shocked embryos examined; compare Fig. 4a and b). However, such segment fusions were also observed at a similar frequency in BTD-expressing homozygous *ems* mutant embryos (32 of 54 embryos examined). Thus, ectopic BTD activity causes metamerization defects independent of *ems* activity. However, BTD-expressing wild-type embryos also develop sclerotic plates (68 cases out of 218 heat-shocked embryos examined; Fig. 4b). In a few cases (11 embryos), segmentation was completely abolished (Fig. 4c), and sclerotic plates were found (Fig. 4c and d). Sclerotic plates were never observed in embryos lacking *ems* activity (16 embryos examined). Thus, their formation in the trunk region of embryos depends on combined BTD and EMS activities. *ems* escapes phenotypic suppression by the HOX-cluster genes without BTD affecting the HOX-cluster gene transcription or translation (Fig. 4e).

The results provide evidence that combined BTD and EMS activities specify the intercalary head segment identity. The gnatho-cephalic homeotic genes *labial* and *Deformed* are normally expressed in intercalary and mandibular head segments, respectively (Fig. 1e; reviewed in ref. 10), and their products cause phenotypic suppression of EMS. As the intercalary segment development is dependent on the regions of BTD which can associate with EMS *in vitro*, it is probable that the EMS–BTD interaction releases the phenotypic suppression. EMS can also overcome phenotypic suppression by the HOX-cluster genes in the trunk when co-expressed with ectopic BTD. We propose that the interaction with BTD allows EMS to relocate from the bottom to the top of the HOX-cluster gene hierarchy. EMS then functions in an anterior-prevalent manner, that is, in the opposite direction to other HOX-cluster genes. The unique homeotic feature of *ems* among the head

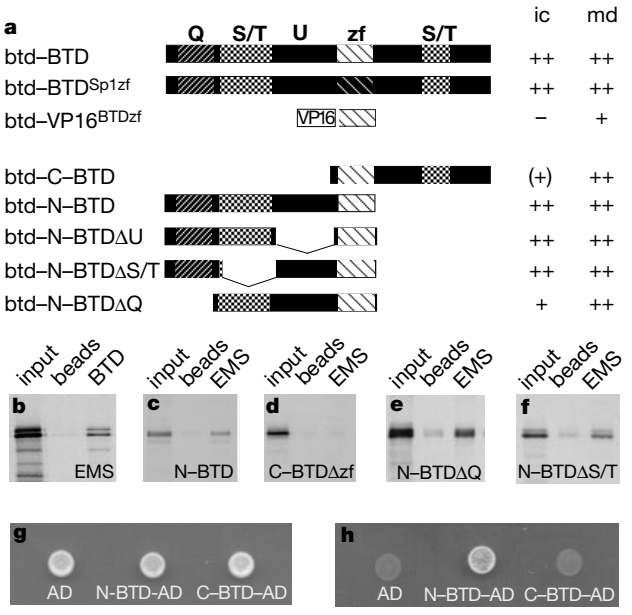

Figure 3 Transgene function in *btd* mutant embryos and interaction between EMS and BTD. **a**, Transgene constructs (left) and rescue of intercalary (ic) and mandibular (md) segments (criteria shown in Fig. 1) of transgene-bearing *btd*-mutant embryos. btd–BTD was reported previously[7,13]. ++, complete rescue of head segments (see Fig. 1a–d) in all embryos ($n \geq 50$); +, partial rescue (subset of segment markers in high penetrance); (–), minimal rescue (a subset of segment markers in low penetrance); –, no rescue. Rescue was independent of the copy number of transgenes, indicating that the rescuing effects were not dose-dependent. zf (hatched boxes), zinc finger region shown to be essential for *btd* function[7]. **b**–**d**, BTD interacts with EMS *in vitro*. [^{35}S]methionine-labelled EMS interacts with Flag-tagged BTD (**b**). Radioactively labelled N terminus of BTD (N–BTD) interacts with EMS (**c**). The C terminus, which lacks the zinc finger domain (C–BTDΔzf) does not bind EMS (**d**). **e**,**f**, N-terminal truncations N–BTDΔQ (**e**) and N–BTDΔS/T (**f**) interact with Flag-tagged EMS. Input refers to 10% of labelled proteins used for the binding reaction; beads refers to unreacted resin with labelled input protein. **g**, **h**, Yeast two-hybrid interactions between EMS and BTD. All yeast clones express the N terminus of EMS (lacking the homeodomain) fused to the GAL4-DNA-binding domain (EMSΔHD–BD). Indicated are the co-transformed GAL4-activation constructs: GAL4-activation domain (AD), N terminus of BTD (including zinc finger region) fused to AD (N–BTD–AD), C-terminal part of BTD (excluding the zinc finger region) fused to AD (C–BTDΔzf–AD). **g**, Growth control on SD/– Leu/– Trp plates. **h**, Interaction assay on SD/– Leu/– Trp/-Ade plates using the stringent nutritional marker system based on an *ADE2* reporter (Clontech). Note that only N–BTD–AD interacts with EMSΔHD–BD.

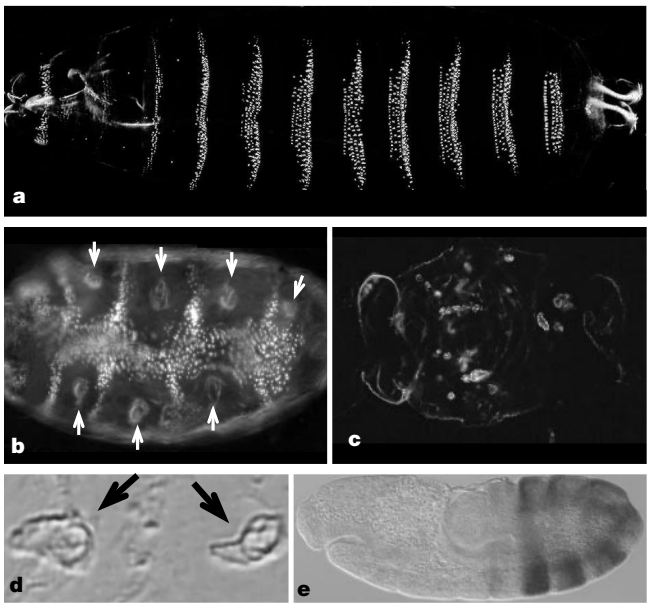

Figure 4 Ectopic *btd* expression lifts phenotypic suppression of *ems*. **a**, Cuticle pattern of a wild-type larva. **b**–**d**, Cuticle patterns of larvae that received heat shock-induced BTD at the time when EMS is expressed in a repeated pattern in the trunk region[8,9]. Note a fusion of segments and the development of sclerotic head plates (arrows in **b**). About 5% of the embryos develop an extreme phenotype showing sclerotic plates (arrows in **d**) in the absence of segments (**c**; enlarged phase contrast micrograph in **d**). **e**, Ectopic BTD does not interfere with the expression of HOX-cluster genes as indicated by the normal pattern of UBX expression in the trunk region of stage 11 embryos. Note that the larvae shown in **b** and **c** are significantly smaller than wild-type larvae.

gap-like genes is therefore consistent with the proposed origin of the gene from the HOX-cluster[3]. By adopting BTD as a partner, EMS could escape phenotypic suppression by gnatho-cephalic HOX gene activities and specify the intercalary head segment identity. □

Methods

Drosophila strains

We used Oregon R, *btd*^{XG}, *svb*^{YP17b} *btd*^{XG} (refs 7,19), homozygous lines of the transgenes described below and hsp70-BTD/hsp70-BTD; ems^{1}/+ for heat-shock experiments in an *ems* mutant background. *svb btd* double mutant was used to identify *btd* mutant cuticles[19].

Generation and analysis of transgenic animals

VP16^{BTDzf}, N–BTD, C–BTD, N–BTDΔU, N–BTDΔS/T and N–BTDΔQ were constructed by polymerase chain reaction (PCR) and standard cloning procedures. N–BTD lacks amino acids 448–644 of the *btd* sequence[7], C–BTD lacks 1–311, N–BTDΔU lacks 240–326 and 448–644, N–BTDΔS/T lacks 116–240 and 448–644, and N–BTDΔQ lacks 6–116 and 448–644. After sequencing, constructs were cloned into a P-element vector providing the 5.2 kilobases (kb) *btd cis*-acting element[13]. btd–EMS contains the 2.2 kb *Xba*I–*Eco*RV fragment of *ems* cDNA[8,9], UAS–EMS contains a 2.2 kb *Eco*RI fragment of *ems* cDNA in pUAST (ref. 15), and hsp70–BTD contains a 3.1 kb genomic *btd Bam*HI fragment in the *Bgl*II site of pCaSpeR-hs (ref. 20).

To generate transgenic flies, constructs were injected in *white* mutant embryos[21]. Except for N–BTDΔQ, at least two independent transgenic lines (balanced over CyO or TM3) were examined. Immunological stainings of embryos[22] were performed with anti-β-galactosidase (Cappel), FP3.38 anti-UBX (ref. 23), 4D9 anti-EN (Developmental Studies Hybridoma Bank; University of Iowa)[22] and 22C10 (ref. 24) primary antibodies using the Vectastain ABC Elite Kit (Vector). Homozygous mutant embryos were identified through blue balancers. Stained embryos were embedded (Canada Balsam, Sigma) or drawn into capillaries. Embryos (30-min collections) were heat-shocked (1 h; 37 °C) after 2 h of development (25 °C). Cuticle preparations[19] and embryos were photographed with a Zeiss Axiophot.

Protein binding assays

Full-length *ems* cDNA[8,9] was cloned into a baculovirus transfer vector[25] to generate a flag-tag fusion construct for overproduction of EMS; the BTD and Sp1 constructs are described[16]. Recombinant baculovirus (Baculogold viral DNA, Pharmingen), expression and purification of Flag-epitope-tagged proteins from Sf9 cells were described[25]. C–BTDΔzf refers to the 880-bp carboxy-terminal *Bgl*I *Ssp*I *btd* fragment cloned into *Pvu*II-digested pRSETB (Invitrogen). For protein interaction studies, about 50 ng of Flag-epitope-tagged proteins (immobilized on Flag-M2 antibody resin; Eastman Kodak) were incubated (3 h, 4 °C) with [^{35}S]methionine-labelled proteins generated by the TNT-coupled *in vitro* transcription/translation system (Promega), washed extensively with 50 mM HEPES, pH 7.9, 25 mM $MgCl_2$, 40% glycerol, 0.8 M KCl, 1% Triton X-100, separated by SDS–PAGE and visualized by autoradiography.

Yeast two-hybrid assays were performed as described (Clontech manuals: Yeast Protocols Handbook; MATCHMAKER Two-Hybrid System 3). EMSΔHD–BD (residues 1–383) was generated by inserting an *Eco*RI/*Bam*HI fragment taken from EMSΔHD–AD into pGBKT7. EMSΔHD–AD was PCR-amplified from *ems* cDNA[8,9] (primers: EMS1F: 5′-CCCGAATTCATGACTAAGACGATTCCG-3′; EMS1R: 5′-CCGCCCGGGCTAG GGCACCAGGAAACTTCC-3′), BTD1–AD (resides 1–217) and BTD2–AD (residues 105–424) were PCR-amplified from *btd* cDNA[7] (primers: BTD1F: 5′-CGCGAATTCATGAT CGATGCGGCCTGC-3′; BTD1R: 5′-GCCGGGCCCTACGCCGCAGCTGCTGCT GCC-3′ and BTD2F: 5′-GCCGAATTCCTATCCGGCTCGAGTTCC-3′; BTD2R: 5′-CGCGGGCCCTAGGCGGCCAGTACCTTCTTGC-3′, respectively). PCR fragments were cloned into *Eco*RI/*Sma*I-digested pGADT7. N–BTD–AD (residues 1–424) was created by opening BTD1–AD with *Stu*I/*Bam*HI and inserting an *Stu*I/*Bam*HI fragment from BTD2–AD. C–BTD–AD (residues 405–645) was PCR-amplified (primers were BTD3F: 5′-GGCGGCATATGAGCGATCACCTCAGC-3′; BTD3R: 5′-CCCGGGCCCATCCTAGG CGGTGGC-3′) and cloned into *Nde*I/*Sma*I-digested pGADT7.

Received 22 February; accepted 29 March 2000.

1. Pankratz, M. & Jäckle, H. in *The Development of Drosophila melanogaster* (eds Bate, M. & Martinez Arias, A.) 467–516 (Cold Spring Harbor Laboratory Press, Cold Spring Harbor, 1993).
2. Martinez Arias, A. in *The Development of Drosophila melanogaster* (eds Bate, M. & Martinez Arias, A.) 517–608 (Cold Spring Harbor Laboratory Press, Cold Spring Harbor, 1993).
3. Manak, J. R. & Scott, M. P. A class act: conservation of homeodomain protein functions. *Dev. Suppl.* 61–77 (1994).
4. Jürgens, G. & Hartenstein, V. in *The Development of Drosophila melanogaster* (eds Bate, M. & Martinez Arias, A.) 687–746 (Cold Spring Harbor Laboratory Press, Cold Spring Harbor, 1993).
5. Cohen, S. M. & Jürgens, G. Mediation of *Drosophila* head development by gap-like segmentation genes. *Nature* **346,** 482–485 (1990).
6. Finkelstein, R., Smouse, D., Capaci, T. M., Spradling, A. C. & Perrimon, N. The *orthodenticle* gene encodes a novel homeo domain protein involved in the development of the *Drosophila* nervous system and ocellar visual structures. *Genes Dev.* **4,** 1516–1527 (1990).
7. Wimmer, E. A., Jäckle, H., Pfeifle, C. & Cohen, S. M. A *Drosophila* homologue of human Sp1 is a head-specific segmentation gene. *Nature* **366,** 690–694 (1993).
8. Dalton, D., Chadwick, R. & McGinnis, W. Expression and embryonic function of *empty spiracles*: a *Drosophila* homeo box gene with two patterning functions on the anterior-posterior axis of the embryo. *Genes Dev.* **3,** 1940–1956 (1989).
9. Walldorf, U. & Gehring, W. J. *Empty spiracles*, a gap gene containing a homeobox involved in *Drosophila* head development. *EMBO J.* **11,** 2247–2259 (1992).
10. Macías, A. & Morata, G. Functional hierarchy and phenotypic suppression among *Drosophila* homeotic genes: the *labial* and *empty spiracles* genes. *EMBO J.* **15,** 334–343 (1996).
11. Lewis, E. B. A gene complex controlling segmentation in *Drosophila*. *Nature* **276,** 565–570 (1978).
12. Duboule, D. & Morata, G. Colinearity and functional hierarchy among genes of the homeotic complexes. *Trends Genet.* **10,** 358–364 (1994).
13. Wimmer, E. A., Cohen, S. M., Jäckle, H. & Desplan, C. *buttonhead* does not contribute to a combinatorial code proposed for *Drosophila* head development. *Development* **124,** 1509–1517 (1997).
14. Gallitano-Mendel, A. & Finkelstein, R. Ectopic *orthodenticle* expression alters segment polarity gene expression but not head segment identity in the *Drosophila* embryo. *Dev. Biol.* **199,** 125–137 (1998).
15. Janody, F., Reischl, J. & Dostatni, N. Persistence of Hunchback in the terminal region of the *Drosophila* blastoderm embryo impairs anterior development. *Development* **127,** 1573–1582 (2000).
16. Schöck, F., Sauer, F., Jäckle, H. & Purnell, B. A. *Drosophila* head segmentation factor Buttonhead interacts with the same TATA box-binding protein-associated factors and *in vivo* DNA targets as human Sp1 but executes a different biological program. *Proc. Natl Acad. Sci. USA* **96,** 5061–5065 (1999).
17. Sadowski, I., Ma, J., Triezenberg, S. & Ptashne, M. GAL4-VP16 is an unusually potent transcriptional activator. *Nature* **335,** 563–564 (1988).
18. Jones, B. & McGinnis, W. The regulation of *empty spiracles* by *Abdominal-B* mediates an abdominal segment identity function. *Genes Dev.* **7,** 229–240 (1993).
19. Wimmer, E. A., Frommer, G., Purnell, B. A. & Jäckle, H. *buttonhead* and *D-Sp1*: a novel *Drosophila* gene pair. *Mech. Dev.* **59,** 53–62 (1996).
20. Thummel, C. S. & Pirotta, V. New pCaSpeR P-element vectors. *Drosoph. Inf. Serv.* **71,** 150 (1992).
21. Rubin, G. M. & Spradling, A. C. Genetic transformation of *Drosophila* with transposable element vectors. *Science* **218,** 348–353 (1982).
22. Patel, N. H. *et al.* Expression of *engrailed* proteins in arthropods, annelids, and chordates. *Cell* **58,** 955–968 (1989).
23. White, R. A. H. & Wilcox, M. Protein products of the Bithorax complex in *Drosophila*. *Cell* **39,** 163–171 (1984).
24. Zipursky, S. L., Venkatesh, T. R., Teplow, D. B. & Benzer, S. Neuronal development in the *Drosophila* retina: monoclonal antibodies as molecular probes. *Cell* **36,** 15–26 (1984).
25. Sauer, F., Hansen, S. K. & Tjian, R. Multiple TAFIIs directing synergistic activation of transcription. *Science* **270,** 1783–1788 (1995).
26. Schmidt-Ott, U., González-Gaitán, M., Jäckle, H. & Technau, G. M. Number, identity, and sequence of the *Drosophila* head segments as revealed by neural elements and their deletion patterns in mutants. *Proc. Natl Acad. Sci. USA* **91,** 8363–8367 (1994).
27. Rogers, B. T. & Kaufman, T. C. Structure of the insect head as revealed by the EN protein pattern in developing embryos. *Development* **122,** 3419–3432 (1996).

Acknowledgements

We thank G. Dowe for sequencing; M. González-Gaitán, G. Vorbrüggen and R. Rivera-Pomar for discussions; C. Klämbt for the 22C10 antibody; and F. Janody and N. Dostatni for the maternal Gal4 driver. The work was supported by the Human Frontier Science Organization (H.J.) and by fellowships of the Fonds der Chemischen Industrie (F.S.), the Alexander-von-Humboldt Stiftung (B.A.P.) and the Boehringer Ingelheim Fonds (J.R.).

Correspondence and requests for materials should be addressed to H.J. (e-mail: hjaeckl@gwdg.de).

Blockade of RAGE–amphoterin signalling suppresses tumour growth and metastases

Akihiko Taguchi*, David C. Blood*, Gustavo del Toro*, Anthony Canet*, Daniel C. Lee*, Wu Qu*, Nozomu Tanji*, Yan Lu*, Evanthia Lalla*, Caifeng Fu*, Marion A. Hofmann*, Thomas Kislinger*, Mark Ingram*, Amy Lu*, Hidekazu Tanaka†, Osamu Hori‡, Satoshi Ogawa ‡, David M. Stern* & Ann Marie Schmidt*

** College of Physicians & Surgeons, Columbia University, New York, New York 10032, USA*
† Osaka University School of Medicine, Osaka 565-0871, Japan
‡ Kanazawa University School of Medicine, Kanazawa 920-8640, Japan

The receptor for advanced glycation end products (RAGE), a multi-ligand member of the immunoglobulin superfamily of cell surface molecules[1–2], interacts with distinct molecules implicated in homeostasis, development and inflammation, and certain diseases such as diabetes and Alzheimer's disease [3–8]. Engagement of RAGE by a ligand triggers activation of key cell signalling